International Journal of Advanced Technology and Engineering Exploration, Vol 11(119)
ISSN (Print): 2394-5443 ISSN (Online): 2394-7454
http://dx.doi.org/10.19101/IJATEE.2024.111100945

Research Article

An analytical study of metal matrix composite materials for railway brake pad applications

Agus Dwi Anggono*, Afif Faishal and Ezza Bayu Aditya
Department of Mechanical Engineering, Universitas Muhammadiyah Surakarta, Kabupaten Sukoharjo, Jawa Tengah 57162, Indonesia

Received: 02-June-2024; Revised: 22-October-2024; Accepted: 24-October-2024

Abstract
Metal matrix composite (MMC) has emerged as a promising engineered material offering unique properties relevant to railway brake pad development. As a critical component of railway braking systems, brake pads necessitate meticulous material selection and development. This study focuses on fabricating MMCs tailored for railway brake pads, comprising a composition of Copper (Cu) 35%, Aluminum (Al) 15%, Iron (Fe) 20%, Magnesium (Mg) 12%, Coconut Charcoal (C) 15%, and Silicon (Si) 3%. Microstructure analysis of brake pad specimens was conducted through scanning electron microscopy (SEM), while wear analysis was performed using the Ogoshi method. Both analyses were conducted post-sintering the specimens at 750°C and normalizing for 12 hours. The results of these analyses were scrutinized to evaluate the suitability of the specimens for implementation as railway brake pads, considering their mechanical and wear properties.

Keywords
Metal matrix composite, Railway brake pads, Microstructure analysis, Wear analysis, Sintering process.

1.Introduction
Brake pads play a vital role in the braking mechanism by transforming kinetic energy into heat via friction, ultimately leading to the deceleration or halting of the vehicle. Slowing down a railway vehicle is intricate and essential for ensuring traffic safety [1]. The complexity stems from the interaction of mechanical, electrical, thermal, pneumatic, and other factors while braking [2]. The selection of brake pad materials is of utmost importance in railway braking systems, as these systems are critical for the safe operation of trains. Typically, brake linings are manufactured using asbestos, semi-metallic, and non-asbestos materials. Asbestos, in particular, produces harmful dust that can adhere to surfaces and be breathed in by individuals, including drivers and bystanders [3]. Not all brake lining materials are suitable for use in various industrial applications owing to concerns regarding environmental contamination and potential health risks [4]. Accordingly, several weaknesses in current brake pad materials encourage us to develop the best brake pad, especially for railway braking systems.

Brake linings are commonly manufactured using various materials, including asbestos, semi-metal, and non-asbestos compositions [5]. However, using asbestos in brake linings poses significant health and environmental risks [6].

Asbestos materials generate toxic dust particles during braking operations, which can adhere to surfaces and dangerously can be inhaled by drivers [7]. Prolonged exposure to asbestos dust is known to cause serious health issues, including respiratory diseases and cancer, particularly among workers in the brake lining industry. Recognizing these hazards, regulatory authorities in many countries, including Indonesia, have imposed bans or restrictions on using asbestos in brake linings [8]. Consequently, there has been a notable shift towards producing brake linings using non-asbestos materials in compliance with these regulations [9]. Non-asbestos brake linings offer comparable performance to asbestos-based linings while mitigating health and environmental risks [10]. This transition towards non-asbestos formulations reflects a commitment to promoting workplace safety and public health, ensuring the well-being of both brake-lining users and industry workers [11].

*Author for correspondence

A composite is a material that combines two or more distinct materials with varying chemical, physical, and mechanical properties [12]. The particle size, shape, and material composition of particles influence the strength of particle composites [13]. This amalgamation creates a new material, exhibiting properties that differ from those of its components. Composites typically consist of two primary constituents: the matrix and the fiber, also known as reinforcement. The matrix is the binder or medium that surrounds and holds the reinforcing fibers together. It provides support, protection, and stability to the composite structure. On the other hand, the fibers, which are embedded within the matrix, contribute to the material's strength, stiffness, and other mechanical properties. By carefully selecting and combining different types of matrices and fibers, engineers can tailor the properties of composites to suit specific applications, resulting in lightweight, durable, and high-performance materials used in a wide range of industries, including aerospace, automotive, construction, and sports equipment manufacturing [14].

Composite materials can be categorized into three primary types according to the matrix metal utilized: polymer matrix composites (PMC), metal matrix composites (MMC), and ceramic matrix composites (CMC) [15]. PMC generally exhibits a lightweight nature and outstanding corrosion resistance, whereas MMC provides superior strength and thermal conductivity. CMC exhibits remarkable resistance to heat and wear. Through the categorization of composites into discrete groups according to the matrix material, engineers and researchers can gain a deeper comprehension of their distinctive characteristics and customize their choices for specific uses. This facilitates the creation of cutting-edge and high-performing materials for diverse industries.

MMC has the potential to be a suitable option for the development of railway brake pads [16]. MMC are utilized in a wide range of automotive and ground transportation applications. MMC is a highly advantageous choice because to its little environmental footprint and great physical characteristics [17]. MMC can demonstrate excellent thermal stability, allowing them to maintain their mechanical properties even at elevated temperatures. This is crucial for brake pads that generate substantial heat during the braking process. On the other hand, some MMC can be challenging to manufacture, particularly those with complex shapes or significant reinforcement content, which can limit their use in specific applications. Designing components with MMC might be more complicated than with traditional materials because the characteristics of MMC can vary based on factors such as the type and amount of reinforcement utilized. It is interesting to research the best composition of MMC for use as a railway brake pad. Several new composites, such as carbon matrix reinforced by carbon fibers, exhibit remarkable high-temperature wear resistance, making them highly desirable for demanding applications. However, they may have limitations in extensive wear scenarios.

Composites like SiCp/Al-Si offer superior properties, including high specific strength, excellent thermal conductivity, and a low coefficient of thermal expansion [18]. Consequently, they are considered ideal MMC for applications such as train braking systems. The composite experiences complex thermal and mechanical loads during braking, generating residual stresses [19]. The strains occur because of the disparity in thermal expansion coefficients between the Sic particles and the Al-Si matrix [20].

In addition, the mechanical forces experienced during braking contribute to fatigue, intensifying the impact of thermomechanical stresses. The significance of comprehending the performance of composites under operational circumstances is emphasized by the cooperative interaction between thermal and mechanical components. The statement emphasizes the necessity of employing innovative techniques in materials design and engineering to enhance the efficiency and longevity of crucial systems such as train braking systems.

This research aims to investigate the results of producing MMC alloy compositions comprising copper (Cu) at 35%, aluminum (Al) at 15%, Fe at 20%, magnesium (Mg) at 12%, carbon (C) at 15%, and silicon (Si) at 3%. The objective is to create composite materials that possess greatly improved mechanical characteristics in comparison to traditional alloys. The research intends to optimize the microstructure and mechanical performance of the MMCs by precisely manipulating the composition and processing parameters. The research aims to clarify the impact of alloy composition on the mechanical properties of the composites by conducting thorough characterization and testing, which includes evaluating tensile strength, hardness, and microstructural analysis. The primary objective is to determine the most favorable combinations of

alloy compositions and processing conditions for manufacturing MMC with exceptional mechanical properties. These composites have the potential to be utilized in a wide range of industries, such as automotive, aerospace, and structural engineering.

This paper explores various aspects of MMC in brake pad applications, starting with the introduction, followed by a literature review in section 2, the research methodology in section 3, results and discussion in section 4 and 5, and the conclusion in section 6.

2.Literature review

MMC have attracted considerable interest in recent years because of their outstanding properties and diverse applications. This literature review seeks to deliver an extensive summary of the existing body of work on MMC, emphasizing their composition, fabrication techniques, and performance attributes. This review aims to analyze the current literature to identify significant gaps in knowledge and explore possible future methods for the advancement of MMC development.

Abhik et al. [21] have previously investigated the mechanical and wear characteristics of MMC consisting of Al and SiC. Brake pads are composed of an Al alloy that is fortified with silicon carbide (SiC) to enhance durability and resistance to wear while taking advantage of the low density of the matrix. Based on wear test investigations, both samples were subjected to abrasion over a range of 100 to 500 cm. Each pass was performed on a completely new abrasive surface, with a distance of 25 cm between each pass. The Al 2014 forms clusters with the SiC reinforcement in an appropriate manner, as evidenced by the surface morphology. Furthermore, the resulting hardness value is significantly lower than that of pure Al specimens, which can be attributed to the reduced sintering time and compaction pressure. Exploring additional studies on the development of Al and SiC composite brake linings would be intriguing. Different research [22] has been carried out on the fabrication of Al7075 MMC incorporating SiC ceramic particles along with various solid lubricants for use in piston development. The study revealed that the composite of Al7075 with 5 wt.% SiC and 5 wt.% graphite exhibited superior mechanical and tribological properties compared to other hybrid composites. This enhancement may be attributed to the synergistic interaction between graphite and the Al7075–SiC MMC. Another investigation indicated outstanding tribological characteristics during stop braking, downhill braking, and parking braking with the Cu-MMCs brake pad [16].

This highlights potential investigations that can be undertaken to enhance the outstanding tribological characteristics. Further investigation is necessary to delve into the fundamental mechanisms of the synergistic interaction between graphite and the Al7075–SiC matrix, which may pave the way for the creation of more advanced hybrid composite materials. Additional investigations have examined the preparation technology, microstructural features, and mechanical properties of SiC particle-reinforced MMC [23]. The investigation revealed that SiC particle-reinforced MMCs are well-suited for automotive applications because of their outstanding properties. Their exceptional specific stiffness, minimal thermal expansion, resistance to wear, ability to withstand heat, and strength at elevated temperatures render them ideal for a range of automotive components. Similar studies have demonstrated that incorporating Si carbide particles into Al matrix composites enhances wear resistance by establishing a structure of robust, load-bearing elements that can withstand abrasion [24]. The encouraging results of this study emphasize the ability of MMCs to transform the automotive sector by providing enhanced materials for various components.

Kumar and Ghosh [25] carried out research on the manufacturing capabilities, development, and performance of MMC for brake pads employing NiSO4 as filler components. The microstructure of the materials is examined by scanning electron microscopy (SEM), while their surface roughness is evaluated using atomic force microscopy (AFM). Under 100X magnification, the SEM test reveals the presence of zircon, brass, potassium titanate, vermiculite, and styrene-butadiene. However, the level of amplification used was not enough to detect any additional compounds that were present in the samples being developed. In addition, Quantitative analysis of AFM images shows that the average values of Ra (0.341 μm) and Rq (0.432 μm) for the brake pads exceed the values on the disc surface. The skewness value shows that the surface roughness distribution is somewhat symmetrical for the brake lining but slightly asymmetrical for the disc. The significance of SEM testing lies in its ability to accurately identify and analyze the microstructure of materials at a high level of detail. This is crucial for comprehending the qualities and performance of

those materials. Another study emphasized on employing diverse nanoparticles to enhance Al composites, particularly via the stir-casting technique [26]. It examines the resultant alterations in the characteristics of these MMCs. The results of this study provide an overview of the fact that the application of Al metal matrix composites (AMMCs) reinforced with nanoparticles has shown significant promise in improving the mechanical and physical properties of materials utilized in aerospace applications. The results provided a strong foundation for future research to explore specific applications, optimize nanoparticle compositions, and investigate the long-term behavior of AMMCs, especially for automotive applications. Additional studies demonstrate that the fabrication process and mechanical behavior of the Al matrix composite reinforced with additively manufactured (AM) 316L stainless-steel (SS) lattice structures offer important insights for the design and development of advanced materials [27]. The integration of AM lattice reinforcement with an Al matrix presents significant potential for use across multiple sectors, including aerospace, automotive, and structural engineering, where there is a growing need for materials that are both lightweight and high-strength.

Lattanzi and Awe [28] conducted a study to examine the impact of Ni, Cu, La, and Ce on the thermophysical characteristics of Al-based MMC. The objective of the study was to utilize enhanced composites for automotive disc brakes. By using alloying materials, the thermal conductivity was reduced by 20% and the stiffness was enhanced by 90% at temperatures up to 470 °C. When there is a need for high stiffness and heat conductivity, using these alloying elements is a suitable solution. The incorporation of various alloying elements improves the properties of brake lining components, making them more attractive for current research purposes. Another investigation utilized a novel enhanced MMC material to enhance the efficiency of a standard car's braking system [29]. Upon thorough analysis of the strength, stiffness, and thermal conditions, the brake disc composed of Al6061/SiC/Gr demonstrates enhanced operational reliability, confirming its safety. The optimized operational reliability shown by the Al6061/SiC/Gr brake disc highlights the possible advantages of integrating hybrid MMC into essential parts of the automotive sector. This suggested the concept of utilizing a hybrid Al, MMC warrants additional investigation in the design and development of other critical components within the braking system.

González-doncel's research [30] encompasses a comprehensive overview of the present state of MMC. The exceptional strength and rigidity of materials, combined with the advantageous mechanical characteristics of metals, such as their remarkable resilience and ability to change shape, make them viable alternatives to metals and other materials currently employed, especially in the transportation industry. MMCs exhibited exceptional strength and rigidity, making them promising alternatives to traditional materials. Hence, the conducted research on MMC is both intriguing and pertinent. Further studies have explored the potential for developing automotive components utilizing MMCs within the automotive industry [31]. Recent advancements in the production of MMC and CMC components, along with the continual emergence of new applications, signify a noteworthy progression in the effort to lower processing and production costs [32].

The subject calls for further examination, as the evolving trends in composites for the automotive industry require a more in-depth analysis. Appart from that, MMC requires specific characteristics to be considered effective. The techniques for fabricating MMCs include powder metallurgy (PM), centrifugal casting, squeeze casting, and stir casting. A significant challenge in the production of MMC is achieving a consistent mixture. Traditional production techniques often necessitate modifications to ensure adequate mixing and yield superior MMCs. Furthermore, various studies have indicated that stir casting stands out as a highly effective method for fabricating MMCs, attributed to its straightforward, reliable process, reduced production costs, and ability to support mass production [33].

This investigation indicates that stir/squeeze casting, powder metallurgy, and semi-solid methods represent the most promising techniques for the production of MMCs. Among them, stir/squeeze casting demonstrates significant effectiveness. The squeezing pressure applied during casting plays a crucial role in determining the mechanical properties of the resulting MMCs. The stir casting process encounters various challenges, including issues with particle distribution, wettability, porosity, stirrer blade erosion, and mixing rate. These challenges also highlight potential avenues for future investigation. This serves as one of the driving forces behind the conduction of this study.

3.Methods

The flowchart for this study is shown in *Figure 1*.

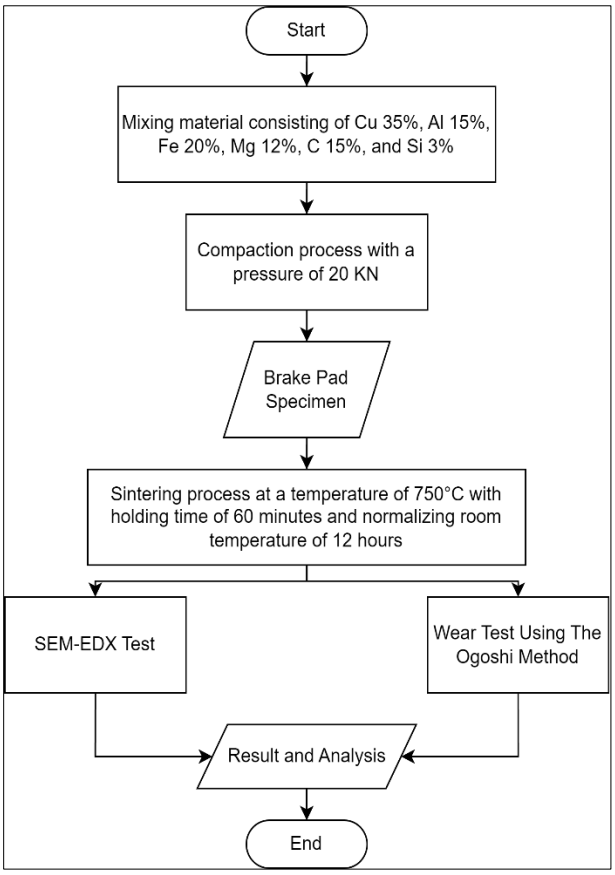

Figure 1 Research flowchart

The methodology used in this study included the formulation of a composite material comprising Cu (35%), Al (15%), Fe (20%), Mg (12%), Coconut Charcoal (C) (15%), and Si (3%). The components were combined meticulously to achieve a uniform composition. The mixture was subsequently compacted at a pressure of 20 kN to create brake pad specimens. Following this, the specimens were subjected to a sintering process at 750°C for a duration of 60 minutes to improve their mechanical properties. Following the sintering process, the specimens underwent a cooling phase to room temperature, which lasted for 12 hours as part of the normalizing procedure. Scanning electron microscope-energy dispersive X-Ray spectroscopy (SEM-EDX) testing was performed to examine the microstructure and elemental composition of the developed brake pads. Furthermore, wear testing was conducted employing the Oghoshi method to assess the wear resistance of the materials.

3.1Mixing materials

For the mixing of powders with specific weights such as Al (0.60 g), Cu (1.40 g), Fe (0.80 g), Mg (0.48 g), C (0.60 g), and Si (0.12 g), the WAB Turbula® T2F Shaker-Mixer is selected. This 3D powder mixer is designed for laboratory-scale applications. The Turbula T2F offers adjustable speed control, ranging from 30 to 100 RPM, allowing precise optimization based on the type of powders being mixed. It also includes a digital timer, ensuring consistent mixing times for each batch. Constructed from stainless steel, the mixer is durable and resistant to contamination, making it suitable for a variety of powders, including metallic and organic compounds. The mixing process is essential in the development of composite specimens. The process guarantees an even distribution of the component materials, comprising the metal matrix and reinforcement particles. A thoroughly blended composition is crucial for attaining the best mechanical properties and avoiding the emergence of unwanted defects, including porosity or segregation. The mixing process significantly impacts the interfacial bonding between the matrix and reinforcement particles, thereby directly affecting the overall strength and durability of the composite.

The composition of the brake lining specimens to be studied is presented in *Table 1*. Once the mixing process is completed, the materials are placed inside the mold. The mixed powder is then carefully filled into a clean, dry mold, compacted incrementally using a hydraulic press. The mold and all tools are thoroughly cleaned with isopropyl alcohol and compressed air to prevent contamination. Gloves are worn during handling, and samples are stored in a dry environment to prevent moisture uptake. After compaction, the sample is carefully removed, inspected for defects, and stored in airtight containers. Before testing, surfaces are cleaned with compressed air, ensuring sample integrity for accurate results.

Table 1 Composition of brake pad specimens

No.	Material	Weight (grams)	Percentage (%)
1	Al	0.60	15
2	Cu	1.40	35
3	Fe	0.80	20
4	Mg	0.48	12
5	C	0.60	15
6	Si	0.12	3
	TOTAL		**100**

3.2Compaction process

For the powder compaction process, the Carver Auto Series Plus Hydraulic Laboratory Press is an ideal choice, offering precise and programmable pressure control. This hydraulic press can achieve a maximum pressure of 30 kN, making it suitable for applying the required 20 kN in increments of 2.5 kN. It features a programmable system that allows for gradual pressure application, holding each 2.5 kN increment for 1 minute and then maintaining the final 20 kN pressure for up to 15 minutes as specified. The press includes a touchscreen interface for easy monitoring and programming of pressure levels and time settings, ensuring precise control over the compaction process. With a 6" x 6" platen size, it provides ample space for various powder compaction dies. The equipment is designed with safety features such as overload protection and an emergency stop function for safe operation. Additionally, it offers an automatic pressure release function after the holding time, and an optional temperature control feature (up to 400°C) for hot pressing applications if needed. This press's rugged construction and compact design make it an excellent choice for laboratory environments, ensuring consistency and accuracy throughout the powder compaction procedure. After compaction, this specimen sample remains very brittle, necessitating heat treatment to enhance its hardness. Specimens from the powder compaction process can be seen in *Figure 2.*

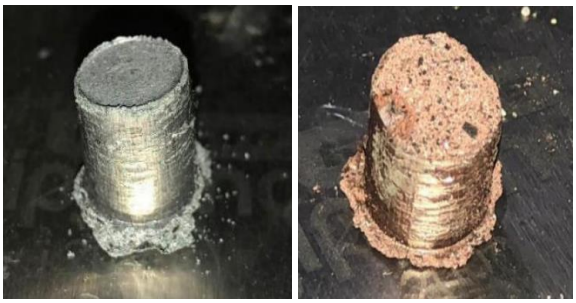

Figure 2 Specimen resulting from the compaction process

3.3Sintering process

For sintering specimens at a temperature of 750°C with a holding time of 60 minutes, the Nabertherm LHT 02/17 LB high-temperature muffle furnace is selected. This furnace is designed for precision and uniformity, with a maximum operating temperature of 1650°C, making it suitable for sintering at various temperatures, including the required 750°C. It features Molybdenum disilicide ($MoSi_2$) heating elements that provide efficient and consistent heating throughout the chamber. The furnace's chamber size is 2 liters, and it includes a PID controller for precise temperature management, ensuring a uniform temperature distribution within ±5°C. The holding time can be programmed accurately, with the furnace capable of maintaining 750°C for up to 99 hours, well beyond the required 60 minutes. Additional features include a digital display for real-time monitoring, rapid heating rates of up to 10°C per minute, and overheat protection for safety. It also includes ventilation ports, allowing for exhaust gas management and controlled atmosphere sintering if necessary. This setup ensures precise, consistent sintering results for specimens.

Throughout the sintering process, the specimen undergoes notable transformations, as depicted in *Figure 3,* resulting in an augmentation of hardness in comparison to its original state before sintering. The increase in hardness can be ascribed to atom diffusion occurring during sintering, resulting in improved interatomic bonding and higher material density. As a result, the sintered specimen demonstrates improved mechanical characteristics, making it better suited for a range of industrial applications that demand exceptional hardness and strength.

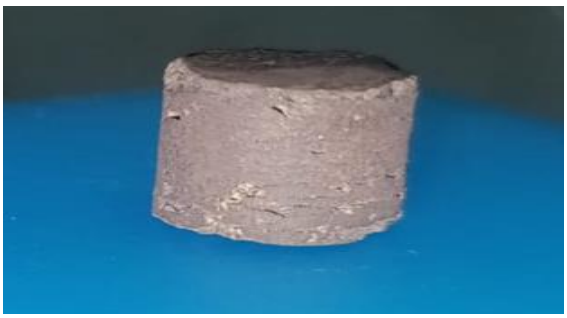

Figure 3 Specimen after sintering process

The sintering process at 750°C is crucial for the formation of composite specimens, as it facilitates atomic diffusion and bonding among the particles. During the sintering process, particles are subjected to elevated temperatures that enable the mobility of atoms at their surfaces. This facilitates the diffusion of atoms and their bonding with adjacent particles, resulting in the creation of a solid, interconnected structure. The sintering process improves the mechanical properties of the composite, resulting in greater strength, hardness, and toughness.

3.4SEM-EDX test

The SEM is a critical tool for material analysis, providing an in-depth view of microstructures and

elemental compositions. It plays an essential role in understanding the intricate details of materials, allowing researchers to assess the degree of uniformity, consistency, and structural integrity. The SEM captures highly detailed images, enabling the examination of surface features, grain boundaries, and other structural components at an extremely fine scale. Proficiency in SEM usage is vital for identifying any anomalies or deviations in material composition that could affect its mechanical, electrical, or thermal properties.

Equipment Details:

- Brand: JEOL JSM-IT500HR Field Emission SEM
- Resolution: 1.5 nm at 30 kV
- Magnification: Up to 1,000,000x
- Features: Equipped with energy dispersive x-ray spectroscopy (EDS) for in-depth elemental analysis and surface characterization of fabricated parts.

In addition to structural imaging, the SEM supports elemental analysis through techniques such as EDS and electron energy loss spectroscopy (EELS). These techniques are crucial for identifying and quantifying the chemical elements within a sample, providing detailed information about its composition. The SEM-EDS/EELS methods accurately detect individual elements and map their spatial distribution on the sample's surface. This capability is especially beneficial for characterizing materials and investigating phenomena like chemical reactions, phase transitions, and contamination.

SEM serves a dual function in material research, offering both visualization and analytical capabilities. Integrating SEM-based microstructural analysis with elemental identification significantly enhances our understanding of material properties, performance, and behavior. This comprehensive approach drives advancements across various fields, including materials science, engineering, and nanotechnology, by providing precise insights into material characteristics and their applications.

3.5Wear test using the Ogoshi method

The Ogoshi method, a well-established approach in materials science for wear testing, is effectively conducted using the Anton Paar TRB³ Pin-on-Disc Tribometer. This tribometer is designed to simulate wear mechanisms under controlled conditions, providing a precise evaluation of the wear resistance of various materials. The equipment supports a maximum load of 60 N, offering flexibility to simulate different contact pressures as required by the Ogoshi method. It features an adjustable rotational speed range from 0.1 to 5000 RPM, allowing accurate control over the sliding speed to replicate diverse wear conditions.

The Ogoshi method for wear testing is a standard procedure widely recognized in materials science and engineering for evaluating the wear resistance of materials. Although not as commonly referenced as other standardized wear tests (e.g., American Standard Testing and Material (ASTM) G99 for the Pin-on-Disc test), the Ogoshi method follows similar principles with specific modifications to suit particular testing needs. This method entails securely affixing the specimen with a pin and delivering a pre-determined force, resulting in controlled frictional engagement between the specimen and a rotating disk. The rotational speed of the disk is predetermined to ensure consistent and replicable testing conditions. When the specimen makes contact with the disk and undergoes both a load and rotational movement, it leads to wear phenomena such as abrasion, adhesion, and surface degradation. The durability and performance attributes of a material can be assessed by evaluating its wear behavior and assessing its rate of degradation. This enables them to assess the material's durability and ability to withstand wear and friction, providing essential information. The Ogoshi method is a reliable and standardized approach employed to evaluate the tribological properties of materials. This technique is widely used in various industries, including automotive, aerospace, and manufacturing.

4.Results

4.1SEM-EDX test

During the SEM-EDX test, the surface of the specimen sample is abraded using sandpaper with different grit sizes (500, 1000, 1500, and 2000) to achieve a polished texture. SEM testing entails collecting high-resolution macroscopic images at a magnification of 610x from four designated sites in order to evaluate the surface condition of the specimen. This allows for the analysis of the distribution of porosity and the identification of chemicals generated as a result of the treatment performed on the specimen samples. The SEM macro photo results are depicted in *Figures 4 to 7*. The area marked by a prominent yellow line in *Figure 4*, covering a significant distance of 48.31 µm, attracts quick focus on the surface of the sample. The specimen's distinctiveness is evident due to its prominent position within the uneven terrain, making

it a central location for observation and examination. The material's heterogeneous nature is emphasized by this unique characteristic, where variations in particle size add to the complexities of its surface morphology. The yellow line in the visual representation clearly reveals the diversity in particle size across the material, providing vital information about its composition and structural features. These findings emphasize the intricate intricacies that are naturally present in the sample, revealing the varied interactions and configurations of its constituent particles.

The detailed examination indicates that smaller particles have not completely filled the empty spaces between the larger particles, resulting in noticeable gaps and abnormalities on the surface. This phenomenon indicates a spatial arrangement in which the smaller particles face difficulties in effortlessly merging with the larger particles. The black arrow is intentionally positioned to attract attention to a specific area where the surface hue is mostly gray. The presence of Al elements in this location is shown by the distinct hue, suggesting a significant and evenly distributed amount of Al across the sample. Thorough observations like this offer significant information on the material's basic components and how they are arranged, which helps us gain a better understanding of its structural properties and possible uses.

In *Figure 5*, the surface of the specimen has a reasonably homogeneous morphological structure, characterized by a regular pattern. However, upon closer scrutiny, it becomes apparent that the distribution of elements is not evenly distributed. Significantly, a 19.76 µm yellow spot stands out, suggesting the existence of Cu elements that are concentrated and do not spread uniformly throughout the surface. This clustering hinders the even distribution, leading to localized abnormalities within the material. In contrast, the red arrow indicates a different region where graphite elements are dispersed in a more regular manner across the surface. The consistent distribution of parts inside the material emphasizes the contrasting behavior of different components and emphasizes the significance of attaining even dispersion for optimal performance and structural integrity.

Figure 6 reveals a highly sophisticated morphological structure that is characterized by several traits and intricacies. The yellow line prominently highlights the existence of holes with different diameters, including a significant void measuring 15.75 µm in diameter. The presence of voids, also known as porosities, is caused by inadequate compaction pressure during the production of the material, which may affect the material's ability to withstand wear. In addition, the black, yellow, and red arrows indicate the location and dispersion of elemental components. The preponderance of Cu elements, indicated by the black arrow, highlights their dominance within the material matrix. In contrast, the yellow arrow signifies the existence of a blend of graphite and Al, whilst the red arrow emphasizes a fusion of Al and Fe components. The elemental compositions of materials have a significant role in determining their overall qualities and performance characteristics. It is crucial to comprehend how these compositions are distributed and interact within the morphological structure.

In *Figure 7*, a conspicuous attribute is accentuated by a crimson striped marking, with a measurement of 20.04 µm, signifying a blend of Cu, Al, and Mg constituents. Simultaneously, a yellow line with a measurement of 11.36 µm indicates the presence of both Fe and Al components. Furthermore, the red arrow clearly denotes the existence of carbon (C). These observations collectively demonstrate the intricate elemental composition and distribution on the surface of the sample. The uneven surface shape and elemental distribution exhibited in *Figure 7* can be attributed to poor mixing or blending of ingredients during the production process. This deficiency leads to specific components not being evenly distributed across the sample, hence causing the observed abnormalities. Therefore, our findings emphasize the significance of precise material processing techniques in order to guarantee the uniform dispersion of elements and improve the overall quality and performance of the material.

SEM-EDX observations were conducted at position 1, focusing on four distinct areas, as illustrated in *Figure 8*. This thorough investigation involves employing a magnification level of 3600x to acquire intricate photos and examine the elemental composition of the sample. The purpose of the SEM-EDX analysis was to obtain detailed information about the surface structure and distribution of elements in the material, with a specific focus on these particular places. The researchers were able to identify specific variations and comprehend the detailed structural features of the specimen more clearly and accurately through this detailed investigation at a high level of resolution.

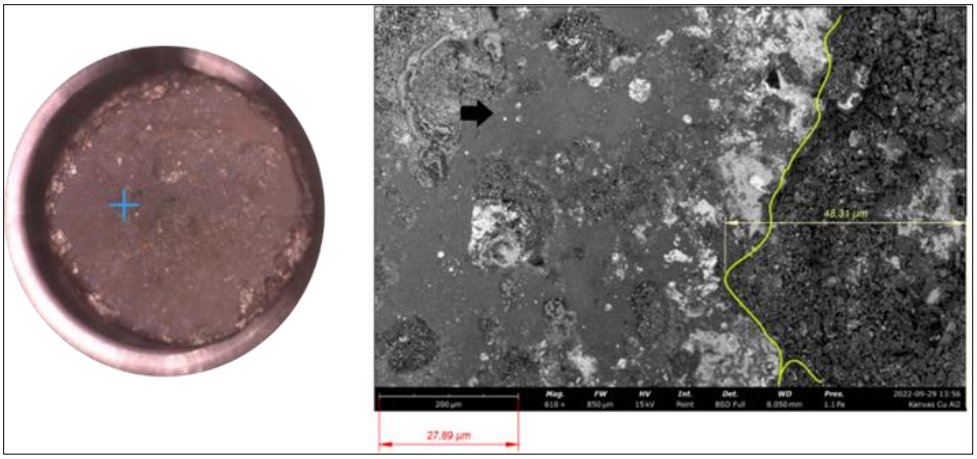

Figure 4 SEM macro photo 610x results at location 1

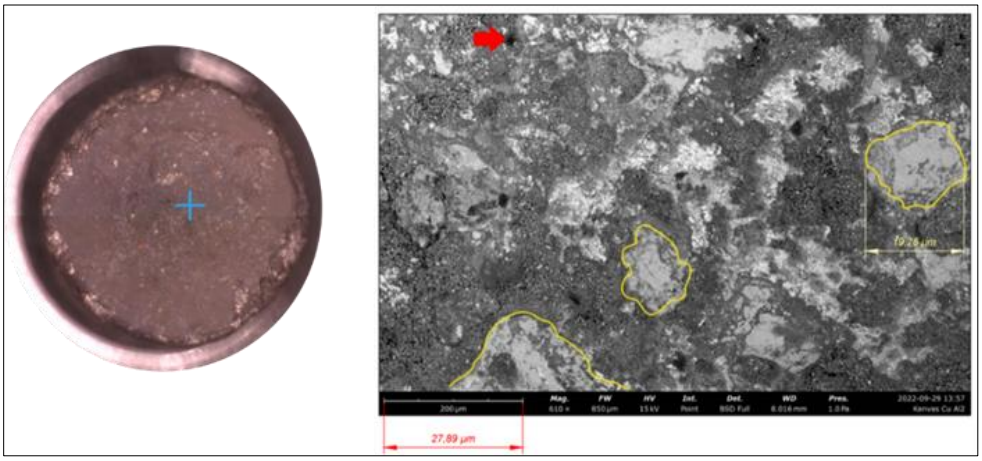

Figure 5 SEM macro photo 610x results at location 2

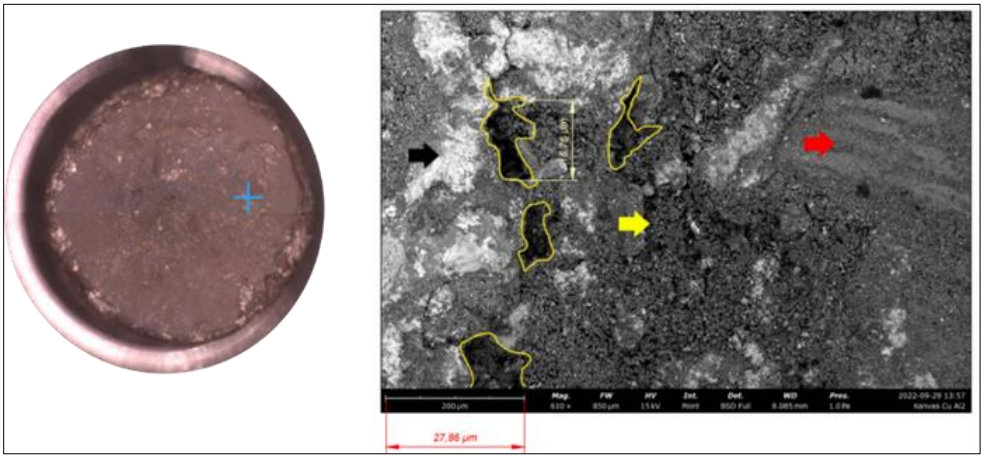

Figure 6 SEM macro photo 610x results at location 3

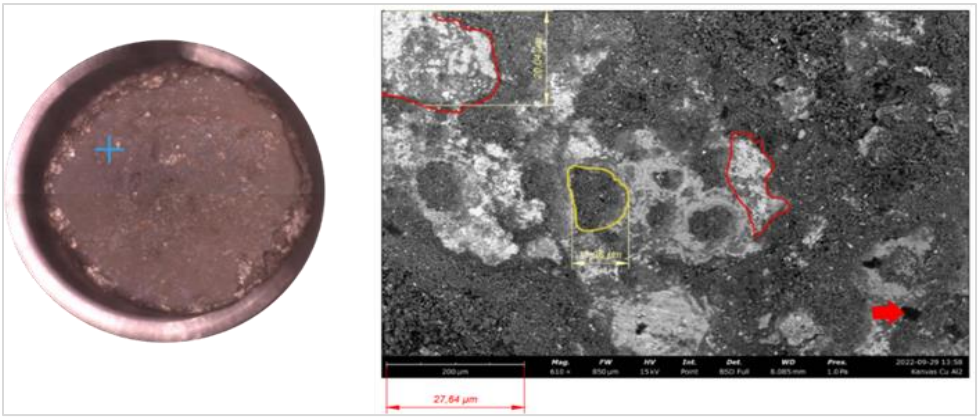

Figure 7 SEM macro photo 610x results at location 4

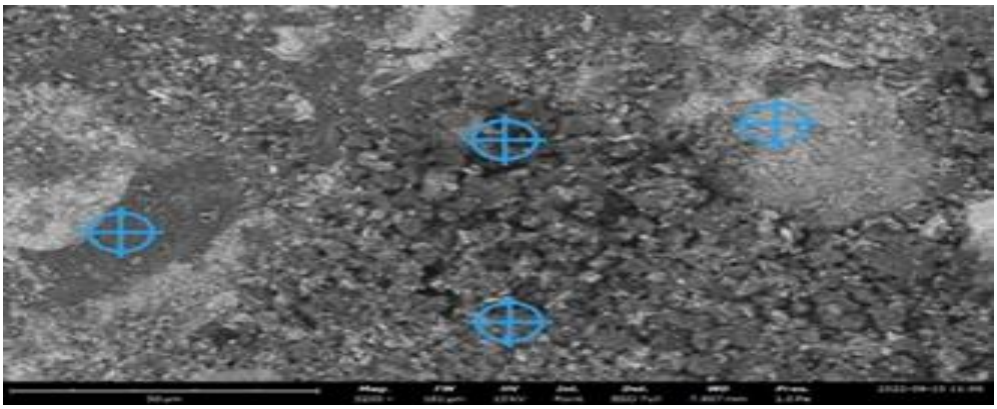

Figure 8 SEM-EDX 3200x results at location 1

Figure 9 depicts the SEM-EDX investigation performed on the surfaces displaying black and gray shades. More precisely, there was a particular location in this area that exhibited a composition where the element C was the main constituent, accounting for 66.2% of the overall composition. In addition, the presence of the Al element was detected at a concentration of 2.5% based on the energy dispersive X-Ray (EDX) data provided in *Table 2*. This examination provides useful insights into the elemental composition of the surfaces being evaluated, emphasizing the abundance of carbon and Al components. It improves our comprehension of the material's qualities and properties. *Figure 10* illustrates the findings of a SEM-EDX examination performed on a surface region that displays a combination of light gray and white colors. In this area, a particular location had a composition that was primarily characterized by the abundance of Fe components, which made up 52.8% of the overall composition. The EDX analysis results presented in *Table 3* have verified the presence of Cu components, constituting 22% of the composition. This comprehensive analysis offers essential observations regarding the fundamental composition of the surface under investigation, emphasizing the notable prevalence of Fe and Cu elements. These findings enhance our comprehension of the qualities and properties of the substance, facilitating subsequent investigation and analysis.

SEM-EDX analysis was conducted on a specific area that exhibited noticeable differences in shades of dark gray and light gray on its surface, as shown in *Figure 11*. The EDX data in *Table 4* reveals that the composition of the specific location in this area consists of 40.2% Al elements, 11% Mg elements, and 8.2% Si components. Interestingly, areas with lighter hues of gray exhibit a higher percentage of Al components. The findings provide crucial insights into the distribution and composition of elements on the surface that was studied, highlighting the substantial presence of Al and its alloys in the material. These discoveries improve our comprehension of the properties and attributes of the material, facilitating further inspection and research.

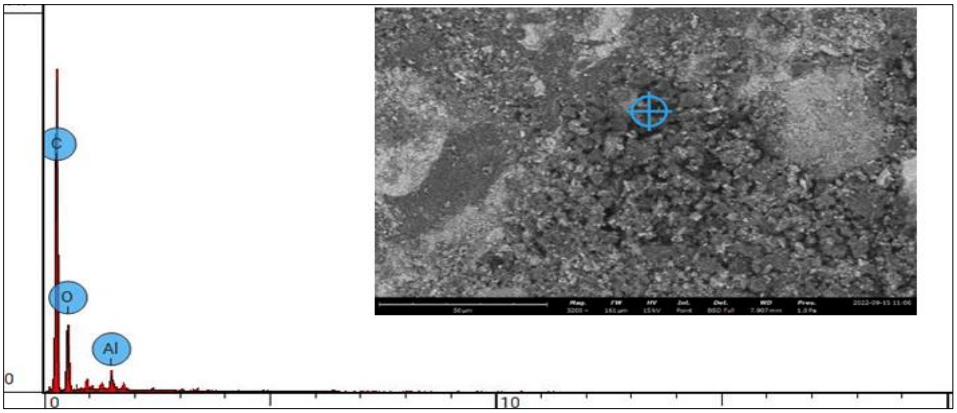

Figure 9 SEM-EDX 3200x results at spot 1 in location 1

Table 2 Elemental composition at spot 1 in location 1

Element number	Element symbol	Element name	Atomic concentration	Weight concentration
6	C	Carbon	72.962	66.266
8	O	Oxygen	25.812	31.231
13	Al	Aluminum	1.227	2.503

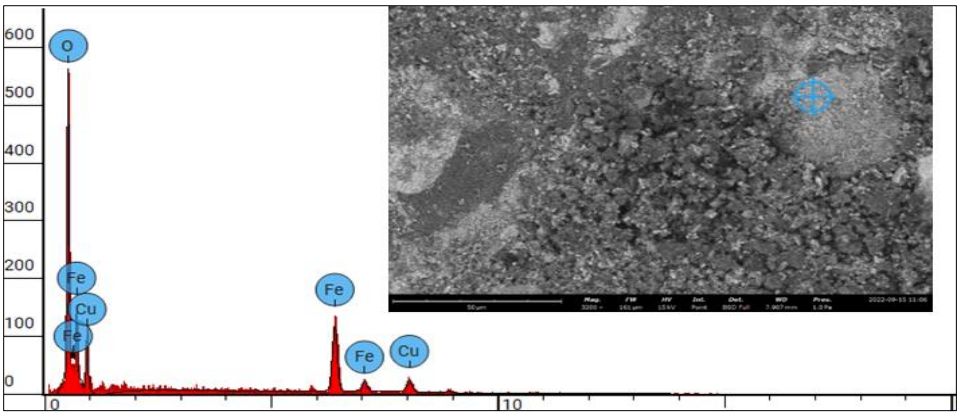

Figure 10 SEM-EDX 3200x results at spot 2 in location 1

Table 3 Elemental composition at spot 2 in location 1

Element number	Element symbol	Element name	Atomic concentration	Weight concentration
8	O	Oxygen	54.943	25.200
26	Fe	Iron	32.979	52.800
29	Cu	Copper	12.078	22.000

Figure 12 illustrates the findings of a SEM-EDX analysis performed on a region exhibiting various hues of dark gray and black on its surface. In this area, there was a particular location with a composition primarily consisting of carbon (C) elements, making up 42.9% of the entire composition. Subsequently, this data can be utilized to cultivate novel technologies, substances, and commodities. Furthermore, it can be utilized to provide information for governmental decisions and legislation. *Table 5* of the EDX data reveals that the Si components have a concentration of 36.2%, while the Fe elements have a concentration of 1.8%. The findings provide vital insights into the distribution and composition of elements on the examined surface, emphasizing the substantial presence of carbon and Si. These discoveries enhance our understanding of the characteristics and qualities of the drug, making it easier to conduct further inquiry and analysis.

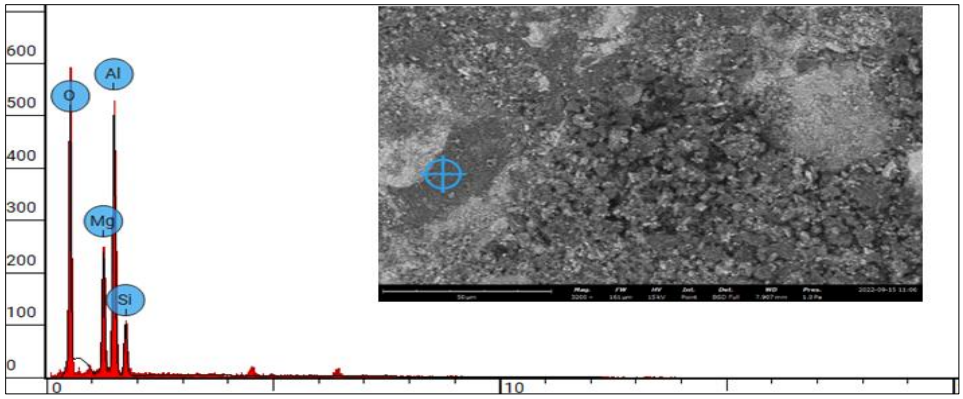

Figure 11 SEM-EDX 3200x results at spot 3 in location 1

Table 4 The element information at spot 3 in location 1

Element number	Element symbol	Element name	Atomic concentration	Weight concentration
8	O	Oxygen	52.172	40.600
12	Mg	Magnesium	9.478	11.000
13	Al	Aluminum	31.233	40.200
14	Si	Silicon	6.117	8.200

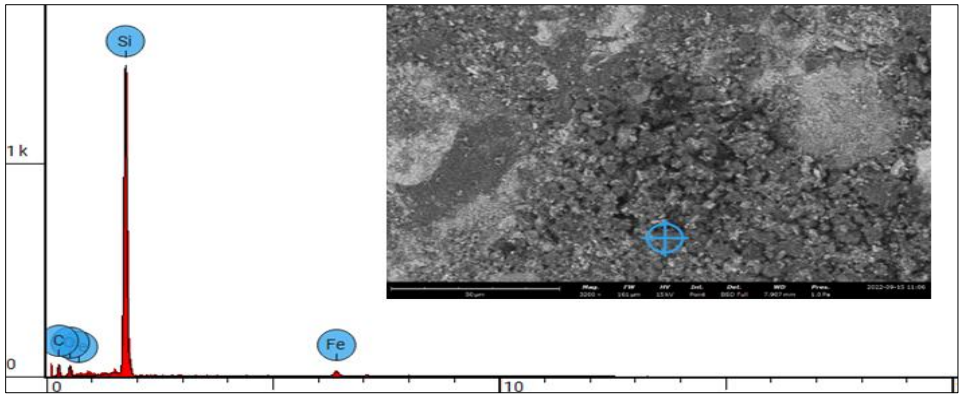

Figure 12 SEM-EDX 3200x results at spot 4 in location 1

Table 5 The element detected at spot 4 in location 1

Element number	Element symbol	Element name	Atomic concentration	Weight concentration
6	C	Carbon	58.811	42.957
8	O	Oxygen	19.403	18.881
14	Si	Silicon	21.227	36.264
26	Fe	Iron	0.559	1.898

Microscopic SEM-EDX analyses were performed at position 2, with particular attention given to three distinct sites, as illustrated in *Figure 13*. This thorough investigation involves using a magnification level of 3600x to capture precise photographs and analyze the elemental composition of the sample. The purpose of the SEM-EDX study was to get extensive data on the surface structure and chemical composition of the material, with specific focus on selected areas of interest. By employing high-resolution analysis, the researchers were able to identify clear differences and develop a more accurate comprehension of the complex structural features of the material. *Figure 14* illustrates the utilization of SEM-EDX analysis on a particular region exhibiting varying tons of white and light gray on its external surface. Within this area, a particular location had a composition predominantly consisting of Cu components, accounting for 69.6% of the total composition. Fe components were detected with a concentration of 10.1% according to the EDX analysis provided in *Table 6*. The data indicates that

locations predominantly characterized by a white color display a greater concentration of Cu components. These observations offer a thorough understanding of the distribution of elements and the composition of the surface being studied. As a result, this makes it easier to conduct further examination and analysis.

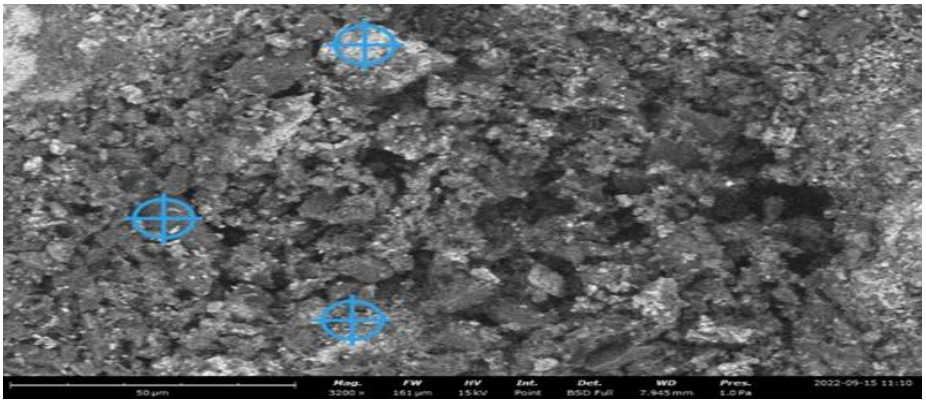

Figure 13 SEM-EDX 3200x results at location 2

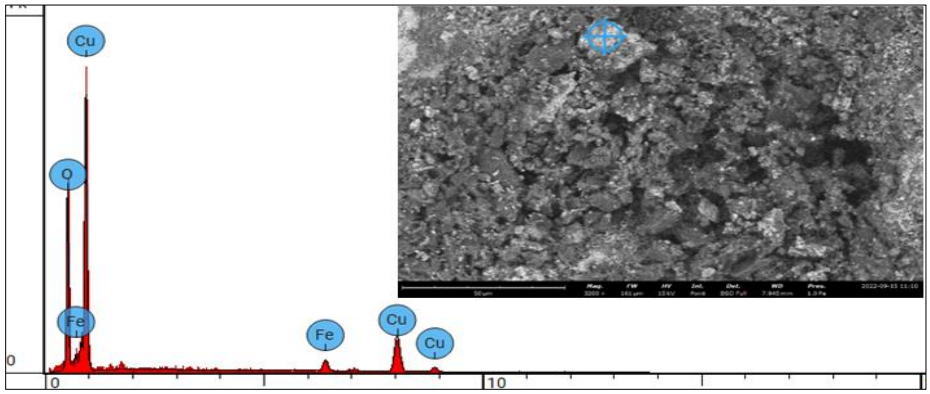

Figure 14 SEM-EDX 3200x results at spot 1 in location 2

Table 6 The element properties at spot 1 in location 2

Element number	Element symbol	Element name	Atomic concentration	Weight concentration
8	O	Oxygen	49.853	20.300
26	Fe	Iron	7.106	10.100
29	Cu	Copper	43.041	69.600

Figure 15 illustrates the application of SEM-EDX analysis on a particular region that exhibits variations in tones of light gray and black on its surface. Within this geographical area, a particular location had a composition predominantly consisting of Si components, accounting for 59.9% of the overall composition. In addition, the analysis conducted using EDX and reported in *Table 7* confirms the presence of carbon (C) components, which make up 34% of the overall composition. The findings offer vital information regarding the elemental composition and distribution of the investigated surface, emphasizing the significant quantities of Si and carbon elements in the material. These insights enhance our understanding of the material's characteristics and properties, facilitating additional investigation and study. A SEM-EDX analysis was performed on a particular region in *Figure 16* that exhibited color variations, notably white and light gray. Within this geographical area, a particular location had a composition predominantly consisting of Si components, accounting for 58.4% of the overall composition. In addition, the EDX analysis in *Table 8* shows that there is a concentration of 11.7% Cu elements and 5.6% Al elements. The findings yield essential data regarding the elemental composition and distribution of the examined surface, emphasizing the significant presence of Si, Cu, and

Al elements in the material. These discoveries enhance our understanding of the characteristics and qualities of the material, facilitating future investigation and analysis.

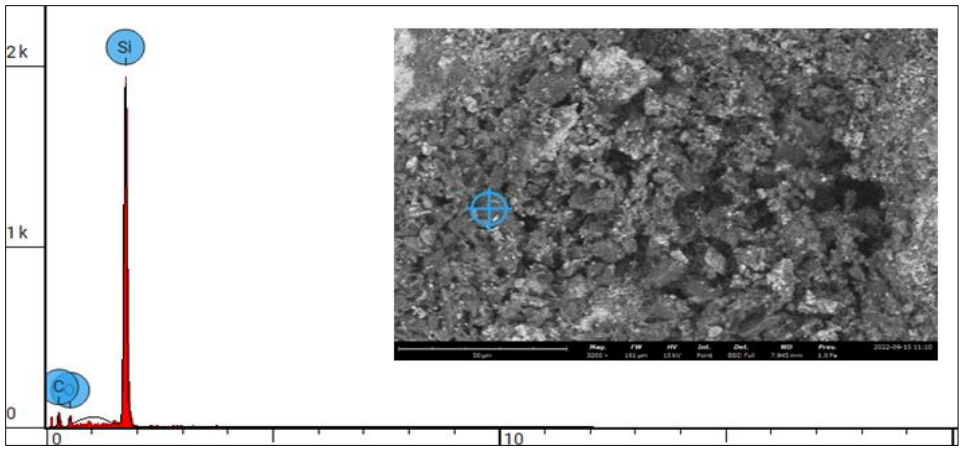

Figure 15 SEM-EDX 3200x results at spot 2 in location 2

Table 7 The element properties at spot 2 in location 2

Element number	Element symbol	Element name	Atomic concentration	Weight concentration
6	C	Carbon	511.968	34.000
8	O	Oxygen	7.133	6.100
14	Si	Silicon	39.898	59.900

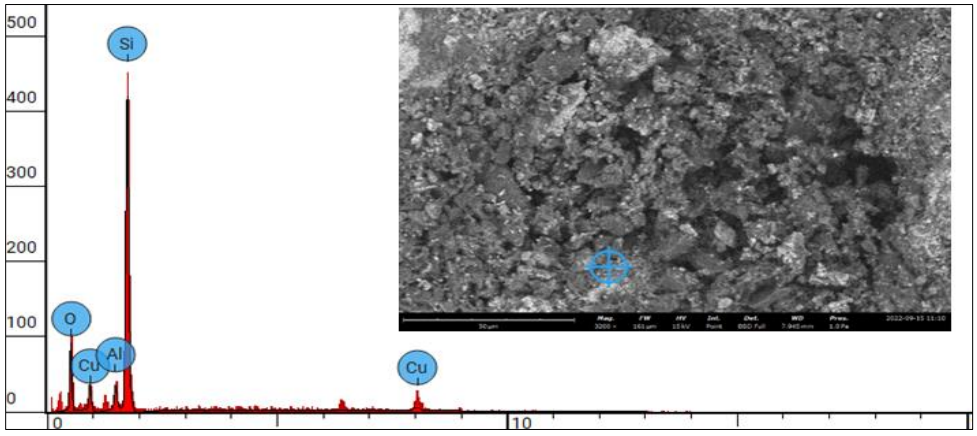

Figure 16 SEM-EDX 3200x results at spot 3 in location 2

Table 8 The elements detected at spot 3 in location 2

Element number	Element symbol	Element name	Atomic concentration	Weight concentration
8	O	Oxygen	38.068	24.300
13	Al	Al	5.205	5.600
14	Si	Silicon	52.112	58.400
29	Cu	Copper	4.615	11.700

The SEM-EDX test results obtained at locations 1 and 2 by micro-observations with a 3200x SEM magnification lead to multiple conclusions. The highest concentration of Al components, comprising 40.2% of the composition, was found at location 1, Spot 3. Location 2, spot 1 was found to have the

highest concentration of Cu, with a composition rate of 69.6%. The black patches exhibited a higher concentration of carbon (C) components, as was noted. location 1, spot 1, had 66.2% carbon (C) and 2.5% Al, while location 1, spot 4, contained 42.9% carbon (C), 36.2% Si and 1.8% Fe. Furthermore,

location 2, spot 2, displayed a composition including 34% carbon and 59.9% Si. The results highlight the elemental compositions seen at various locations during the SEM-EDX analysis, providing valuable information about the characteristics and composition of the material in distinct areas.

4.2Wear test

The wear testing methodology followed the guidelines outlined in the ASTM G 99-04 test standard, employing the Ogoshi method to assess the material's resistance to wear. By employing this standardized approach, consistency and accuracy are ensured while evaluating the properties of deterioration in different materials and under diverse testing conditions. The wear test results yielded comprehensive data that was meticulously documented and shown in *Table 9*. This table provides essential data on the material's response to wear-induced pressures, offering vital insights into its durability, frictional properties, and overall mechanical performance. By rigorously following established testing protocols and meticulously recording test results, researchers can get valuable knowledge about the durability characteristics of materials. This facilitates well-informed decision-making and enhances the optimization of material design and manufacturing processes.

The wear value obtained from the wear test, computed using the data shown in *Table 9*, is 2.45424E-06. The value is determined by evaluating various parameters throughout the testing process. The specifications for this experiment are as follows: The measured wear width on the test specimen (b0) is 2.2973 mm. The width of the wear disk (b) is 3 mm, with a radius of 13.12 mm. The pressure force applied during the wear process (p0) is 2.12 kg, and the distance traveled by the wear process (l0) is 66.6 mm. The wear value is a crucial measure of the material's wear resistance, with lower values indicating higher resistance to wear. Furthermore, it is well acknowledged that the hardness of the specimen plays a vital role in determining its capacity to withstand wear. In general, specimens with greater hardness exhibit improved resistance to wear. Thus, the results obtained from the wear test emphasize the importance of hardness as a critical factor that influences the material's wear performance.

Table 9 Wear test result

Specimen code	**Copper (Cu Al)**
b0(mm)	2,2973
b(mm)	3
r(mm)	13,12
p0(kg)	2,12
l0(m)	66,6
Specific Wear (Ws) (mm^2/kg)	2,45424 E-06

5.Discussion

5.1SEM-EDX test of brake pad specimens

The SEM-EDX test required using sandpaper with different grit sizes (500, 1000, 1500, and 2000) to abrade the surface of the specimen and obtain a polished texture. High-resolution macroscopic images were obtained at a magnification of 610x from four distinct areas in order to assess the surface condition. *Figure 4* displays a strong yellow line that spans 48.31 µm. This line highlights the material's heterogeneous nature, indicating differences in particle size and intricate surface morphology. These observations suggest that smaller particles did not fully occupy the gaps between bigger ones, leading to visible gaps. An arrow, colored black, indicated a region that was gray in color, indicating the likely presence of Al. This highlights the need to study the distribution of elements in order to get insight into the structural characteristics and possible uses of the material.

Upon closer analysis of *Figures 5* and *6*, disparities in the distribution of elements and morphological structures were observed. *Figure 5* displayed a surface that was mostly uniform but with an irregular distribution of elements, notably a 19.76 µm yellow patch suggesting a high concentration of Cu. On the other hand, graphite elements were distributed more uniformly. *Figure 6* illustrates an intricate morphological configuration with empty spaces resulting from insufficient compaction pressure, which negatively impacts the ability to withstand wear. The elemental mapping revealed the prevalence of Cu and combinations of graphite, Al, and Fe. *Figure 7* provides a comprehensive analysis of the distribution of several elements, including Cu, Al, Mg, Fe, and carbon, using special markers to indicate their blends. These findings highlight the significance of accurate material processing methods in order to achieve consistent distribution of elements and improve the quality and performance of the material.

The SEM-EDX analysis was performed at position 1, specifically examining four unique locations at a magnification of 3600x to thoroughly investigate the elemental makeup of the sample. The purpose of this investigation was to offer a thorough examination of the surface composition and spatial arrangement of

elements. *Figure 8* emphasized these particular regions, enabling researchers to discern differences and gain a more precise understanding of the intricate structural characteristics of the material. *Figure 9* displayed a surface featuring black and gray tones, indicating a composition mostly consisting of carbon (66.2%) and Al (2.5%). This highlights the elemental makeup and qualities of the material.

Additional insights into the material's composition were obtained by further investigation of *Figures 10, 11, and 12*. *Figure 10* revealed a surface area exhibiting a combination of light gray and white hues, distinguished by a significant presence of Fe (52.8%) and Cu (22%). *Figure 11* depicts an area characterized by contrasting dark and light gray tones, indicating a notable abundance of Al (40.2%), Mg (11%), and Si (8.2%). *Figure 12* analyzed a region characterized by dark gray and black colors, revealing a composition consisting mainly of carbon (42.9%) and Si (36.2%). The findings emphasize the diverse distribution and composition of elements in different surface areas, enhancing our comprehension of the material's properties and enabling further research and development.

Microscopic SEM-EDX studies were performed at position 2, specifically examining three separate locations indicated in *Figure 13*, with a magnification level of 3600x. The purpose of this high-resolution investigation was to collect comprehensive data on the surface structure and chemical composition of the material, specifically focusing on certain areas of interest. In *Figure 14,* a region with different shades of white and light gray is emphasized. Cu components make up 69.6% of the entire composition, while Fe accounts for 10.1%. These findings offer a comprehensive comprehension of the distribution of elements, specifically highlighting the significant abundance of Cu in white-colored regions, which facilitates more research and investigation. *Figure 15* examined a specific area characterized by light gray and black shades, uncovering a composition primarily composed of Si (59.9%) and carbon (34%). *Figure 16* analyzed a region characterized by white and light gray colors, revealing notable proportions of Si (58.4%), Cu (11.7%), and Al (5.6%) elements. These findings improve our comprehension of the material's constituent composition and distribution, highlighting the significant abundance of Si, Cu, and Al.

The SEM-EDX investigations conducted at locations 1 and 2, using a magnification of 3200x, reveal diverse elemental compositions. These findings offer useful insights into the features and qualities of the material in distinct regions. Location 1, spot 3 had the highest concentration of Al (40.2%), whereas location 2, spot 1 had the highest concentration of Cu (69.6%). Other places showed significant amounts of carbon and Si, indicating a varied composition of elements in the material.

The presence of elements like Cu and Si significantly enhances the mechanical properties, such as hardness and wear resistance, in MMCs. Cu improves thermal conductivity and strength by forming hard intermetallic compounds, which enhances hardness and resistance to deformation. Si, often used as SiC, acts as a reinforcing agent, increasing hardness and wear resistance through the formation of stiff particles that strengthen the matrix and reduce porosity. These particles provide a robust barrier against abrasion, resulting in improved performance under sliding wear conditions.

Microstructural features like porosity and particle distribution directly influence these properties. Reduced porosity and uniform particle distribution lead to higher hardness values, as a compact microstructure minimizes weak points and increases density. In real-world applications, such as railway brake pads, a well-distributed and dense microstructure ensures stability and efficiency under high temperatures and friction, critical for maintaining wear resistance and durability under mechanical and thermal stress.

Based on the SEM-EDX observations and wear test results, several wear mechanisms, including abrasion and adhesion, are identified. The SEM-EDX analysis revealed uneven particle distribution, porosity, and elemental clustering, which are critical factors contributing to these mechanisms. For instance, areas with concentrated Cu particles and irregular morphology indicate higher abrasion resistance, as these hard particles act as barriers against sliding wear. However, regions exhibiting porosity or gaps between larger and smaller particles may be prone to adhesive and fatigue wear due to insufficient compaction pressure during processing, leading to weak bonding and structural inconsistencies.

The wear test results align with the SEM-EDX findings, showing that areas with higher hardness values, correlating with Cu and Si presence, demonstrated better wear resistance, particularly against abrasion. In contrast, areas with high porosity

or uneven distribution of reinforcing elements like Si and Al exhibited higher wear rates, supporting the notion that inadequate compaction affects the material's ability to withstand real-world conditions, such as repeated stress or sliding. Thus, optimizing the microstructure by ensuring uniform particle dispersion and minimizing porosity is crucial for enhancing the wear performance of such composites.

5.2Wear test result of brake pad specimens

The wear testing methodology followed the ASTM G 99-04 test standard and used the Ogoshi method to assess the resistance of the material to wear. This standardized methodology guarantees uniform and precise evaluations of material decay under different testing circumstances. The wear tests yielded extensive data that was thoroughly recorded in *Table 9*, offering vital insights into the material's durability, frictional characteristics, and overall mechanical performance. Researchers can acquire significant insights into material durability by adhering strictly to established protocols and meticulously documenting data. This enables informed decision-making and improves the optimization of material design and production processes. The wear test resulted in a wear value of 2.45424E-06, which was calculated by analyzing different factors. These data include a wear width of 2.2973 mm on the test specimen, a wear disk width of 3 mm, a wear disk radius of 13.12 mm, an applied pressure force of 2.12 kg, and a wear process distance of 66.6 mm. The wear value is crucial in evaluating the resilience of materials to wear, where lower values indicate greater resistance. The test results further emphasize the significance of specimen hardness, since harder materials typically demonstrate superior wear resistance. Therefore, the results highlight the important impact of hardness on the wear performance of a material.

The processing parameters, such as compaction pressure and sintering temperature, significantly influence the microstructure and material properties observed in the specimens. The compaction process involved gradual pressure increments up to 20 kN, ensuring the powder particles were densely packed. Higher compaction pressure minimizes porosity, leading to increased density and improved mechanical strength. Insufficient pressure, however, can result in voids and inconsistent particle distribution, as observed in some SEM images showing gaps between particles, which could reduce wear resistance and durability. The sintering temperature, set at 750°C, facilitates atomic diffusion, enhancing the interparticle bonding and overall hardness of the material. SEM-EDX analyses revealed that regions with improved density and fewer voids exhibited higher hardness and wear resistance, consistent with the effective sintering conditions. Regarding surface preparation, using different grit sizes (500, 1000, 1500, and 2000) significantly impacts SEM-EDX results. Finer grit sizes provide smoother surfaces, reducing artifacts and revealing more precise particle distributions and element mapping. In contrast, coarser grits may leave surface irregularities that interfere with accurate compositional analysis, affecting the interpretation of microstructural features.

5.3Study limitations and comparative analysis

One of the primary limitations of the study is the variation in compaction pressure and sintering temperature control. Inadequate or inconsistent application of pressure during compaction can lead to porosity, as seen in some SEM-EDX observations, where voids were present, weakening the overall structure. Additionally, maintaining uniform sintering temperatures is crucial; deviations can cause uneven diffusion of elements and result in inconsistent mechanical properties. Another limitation is the surface preparation process; using different grit sizes for polishing may introduce variability in surface texture, potentially affecting the accuracy of the SEM-EDX analysis and leading to discrepancies in understanding the material's microstructure. In comparison to similar studies [17,21,25,28] on MMCs for brake pad applications, the current research showed enhanced wear resistance with optimized Cu and Si compositions, aligning with findings from other works using hybrid MMCs. However, differences in compaction techniques, such as the use of higher or more controlled pressures in other studies, have demonstrated even more uniform particle distribution and lower porosity levels, leading to improved hardness and wear performance. While the current study employed a standard sintering temperature of 750°C, other research showed that higher temperatures (up to 800°C) with extended holding times could yield even greater diffusion and bonding of particles [23]. To further validate the findings, future studies could explore these varied compaction and sintering conditions to optimize the material properties fully.

A complete list of abbreviations is listed in *Appendix I.*

6.Conclusion and future work

SEM examination initially indicated that the surface density of the specimen sample is nearing its maximum capacity, with only a small number of visible voids. This implies that the current load application, compaction, and sintering actions meet the required parameters. Furthermore, a higher compaction pressure increases the density by efficiently filling the gaps between particles in the sample. The EDX test findings indicated partial composition in certain areas, potentially due to inadequate mixing or blending methods. In addition, the wear test results showed a value of 2.454×10^{-6} mm^2/Kg, which is significantly lower than the wear value prescribed by the Indonesian National Standard (SNI) of 5×10^{-4} mm^2/Kg to 4×10^{-3} mm^2/Kg. These findings suggest the need for further optimization and refinement in the material production process to meet the required wear standards set by regulatory bodies.

Acknowledgment

We gratefully acknowledge the financial support for this research through contract number 0258.792/I.3/D/2024 under the National Research of Muhammadiyah, batch VII 2024 scheme. This funding has been instrumental in enabling us to conduct our investigation and advance our understanding of the field. We sincerely thank the National Research of Muhammadiyah for their invaluable contribution to our project.

Conflicts of interest

The authors have no conflicts of interest to declare.

Data availability

The data utilized in this research were gathered from the outcomes of testing and specimen preparation at Universitas Muhammadiyah Surakarta, Indonesia. The data is not accessible to the public. Nonetheless, the corresponding author can make the data available upon a reasonable request.

Author's contribution statement

Agus Dwi Anggono: Conceptualized the study, designed the experiments, conducted the statistical analysis, and contributed to interpreting the data. **Afif Faishal:** Contributed significant insights to the theoretical framework and contributed to the manuscript construction. **Ezza Bayu Aditya:** Prepared the specimens and gathered the test data. All authors examined and sanctioned the final version of the manuscript.

References

[1] Günay M, Korkmaz ME, Özmen R. An investigation on braking systems used in railway vehicles. Engineering Science and Technology, an International Journal. 2020; 23(2):421-31.

[2] Saha D, Sharma D, Satapathy BK. Challenges pertaining to particulate matter emission of toxic formulations and prospects on using green ingredients for sustainable eco-friendly automotive brake composites. Sustainable Materials and Technologies. 2023: e00680.

[3] Vijay R, Rajan BS, Sathickbasha K, Hariharasakthisudhan P, Singaravelu DL, Manoharan S, et al. Influence of metal sulfide coated steel fibers on the friction and wear performance of brake friction composites. Tribology International. 2022; 176:107924.

[4] Ayogwu DO, Sintali IS, Bawa MA. A review on brake pad materials and methods of production. Composite Materials. 2020; 4(1):8-14.

[5] Purboputro PI, Darmawan AS. The effect of copper particles size on hardness, wear resistance and friction coefficient of fiberglass-carbon particles-copper particles reinforced composite. In materials science forum 2021 (pp. 49-55). Trans Tech Publications Ltd.

[6] Yigrem M, Fatoba O, Tensay S. Tensile strength, wear characteristics and numerical simulation of automotive brake pad from waste-based hybrid composite. Materials Today: Proceedings. 2022; 62:2954-64.

[7] Darmawan AS, Purboputro PI, Febriantoko BW, Hamid A. Effect of pressure to rice plant fibre reinforced composite on coefficient of friction of brake lining. In IOP conference series: materials science and engineering 2020 (pp. 1-5). IOP Publishing.

[8] Ekpruke E, Ossia CV, Big-alabo A. Recent progress and evolution in the development of non-asbestos based automotive brake pad-a review. Journal of Manufacturing Engineering. 2022; 17(2):51-63.

[9] Ademoh NA, Olabisi AI. Development and evaluation of maize husks (asbestos-free) based brake pad. Development. 2015; 5(2):67-80.

[10] Bachchhav BD, Hendre KN. Wear performance of asbestos-free brake pad materials. Jordan Journal of Mechanical & Industrial Engineering. 2022; 16(4):459-69.

[11] Adeyemi IO, Nuhu AA, Thankgod EB. Development of asbestos-free automotive brake pad using ternary agro-waste fillers. Development. 2016; 3(7):5307-23.

[12] Bhong M, Khan TK, Devade K, Krishna BV, Sura S, Eftikhaar HK, et al. Review of composite materials and applications. Materials Today: Proceedings. 2023.

[13] Darmawan AS, Purboputro PI, Febriantoko BW. The aluminum powder size'effect on rice plant fiber reinforced composite to hardness, wear and coefficient of friction of brake lining. In conference series: materials science and engineering 2020 (pp. 1-9). IOP Publishing.

[14] Purboputro PI, Darmawan AS, Febriantoko BW. Effect of operation conditions to rice plant fiber reinforced composite on coefficient of friction and wear rate of brake lining. In conference series: materials science and engineering 2020 (pp. 1-6). IOP Publishing.

[15] Zhang X, Chen Y, Hu J. Recent advances in the development of aerospace materials. Progress in Aerospace Sciences. 2018; 97:22-34.
[16] Xiao Y, Zhang Z, Yao P, Fan K, Zhou H, Gong T, et al. Mechanical and tribological behaviors of copper metal matrix composites for brake pads used in high-speed trains. Tribology International. 2018; 119:585-92.
[17] Chatterjee A, Sen S, Paul S, Roy P, Seikh AH, Alnaser IA, et al. Fabrication and characterization of SiC-reinforced aluminium matrix composite for brake pad applications. Metals. 2023; 13(3):1-17.
[18] Ren S, He X, Qu X, Li Y. Effect of controlled interfacial reaction on the microstructure and properties of the SiCp/Al composites prepared by pressureless infiltration. Journal of Alloys and Compounds. 2008; 455(1-2):424-31.
[19] Li W, Chen ZH, Chen D, Teng J, Fan C. Low-cycle fatigue behavior of SiCp/Al–Si composites produced by spray deposition. Materials Science and Engineering: A. 2010; 527(29-30):7631-7.
[20] Xu Q, Ma A, Wang J, Sun J, Jiang J, Li Y, et al. Development of high-performance SiCp/Al-Si composites by equal channel angular pressing. Metals. 2018; 8(10):1-13.
[21] Abhik R, Umasankar V, Xavior MA. Evaluation of properties for Al-SiC reinforced metal matrix composite for brake pads. Procedia Engineering. 2014; 97:941-50.
[22] Devaganesh S, Kumar PD, Venkatesh N, Balaji R. Study on the mechanical and tribological performances of hybrid SiC-Al7075 metal matrix composites. Journal of Materials Research and Technology. 2020; 9(3):3759-66.
[23] Wang Y, Monetta T. Systematic study of preparation technology, microstructure characteristics and mechanical behaviors for SiC particle-reinforced metal matrix composites. Journal of Materials Research and Technology. 2023; 25:7470-97.
[24] Gultekin D, Uysal M, Aslan S, Alaf Mİ, Guler MO, Akbulut H. The effects of applied load on the coefficient of friction in Cu-MMC brake pad/Al-SiCp MMC brake disc system. Wear. 2010; 270(1-2):73-82.
[25] Kumar S, Ghosh SK. Porosity and tribological performance analysis on new developed metal matrix composite for brake pad materials. Journal of Manufacturing Processes. 2020; 59:186-204.
[26] Qadir J, Lewise AS, Wessley GJ, Samuel GD. Influence of nanoparticles in reinforced aluminium metal matrix composites in aerospace applications–a review. Materials Today: Proceedings. 2023.
[27] Hamada A, Mansour EH, Jaskari M, Abd-elaziem W, Mohamed AK, Elshokrofy H, et al. Strengthening aluminum matrix composite with additively manufactured 316L stainless steel lattice reinforcement: processing methodology, mechanical performance and deformation mechanism. Journal of Materials Research and Technology. 2024; 29:1087-101.
[28] Lattanzi L, Awe SA. Thermophysical properties of Al-based metal matrix composites suitable for automotive brake discs. Journal of Alloys and Metallurgical Systems. 2024; 5:100059.
[29] Singh M, Garg HK, Maharana S, Muniappan A, Loganathan MK, Nguyen TV, et al. Design and analysis of an automobile disc brake rotor by using hybrid aluminium metal matrix composite for high reliability. Journal of Composites Science. 2023; 7(6):1-12.
[30] González-doncel G. An overview of metal matrix composites, MMCs, and future perspectives. In: caballero FG, editor. encyclopedia of materials: metals and alloys, Oxford: Elsevier; 2022 (pp.141-6).
[31] Singh H, Brar GS, Kumar H, Aggarwal V. A review on metal matrix composite for automobile applications. Materials Today: Proceedings. 2021; 43:320-5.
[32] Singh P, Raghavender V, Joshi S, Vasant NP, Awasthi A, Nagpal A, et al. Composite material: a review over current development and automotive application. Materials Today: Proceedings. 2023.
[33] Ramanathan A, Krishnan PK, Muraliraja R. A review on the production of metal matrix composites through stir casting-furnace design, properties, challenges, and research opportunities. Journal of Manufacturing Processes. 2019; 42:213-45.

Agus Dwi Anggono was born on June 17, 1976, in Kudus, Central Java. He is an Associate Professor in the Department of Mechanical Engineering at Universitas Muhammadiyah Surakarta. He earned his bachelor's degree from Universitas Muhammadiyah Surakarta in 1999, followed by a master's degree in Mechanical Engineering from Universitas Gadjah Mada in 2009. In 2014, he completed his doctorate at Universiti Tun Hussein Onn. His research interests include Advanced Materials, Nanofluids, Nanomaterials, Manufacturing, Finite Element Analysis, and Reverse Engineering.
Email: ada126@ums.ac.id

Afif Faishal was born on June 29, 1997 in Yogyakarta's Special Region. In 2019, he received a bachelor of Mechanical Engineering degree from Universitas Muhammadiyah Surakarta, Indonesia. Then, he received a master of Mechanical Engineering degree from Universitas Sebelas Maret Surakarta, Indonesia. Since 2024, he has been a lecturer in the Mechanical Engineering department, faculty of engineering, Universitas Muhammadiyah Surakarta. Renewable Energy, Biomass, Municipal Solid Waste, Gasification, Energy Conversion, Environmental Engineering, and Energy Sustainability are among his research interests.
Email: af515@ums.ac.id

Ezza Bayu Aditya was born on July 18, 2000 in Kudus, Jawa Tengah. In 2023, he received a bachelor of Mechanical Engineering degree from Universitas Muhammadiyah Surakarta, Indonesia. Health, Safety and Environment, Mechanical, Manufacturing, and Materials Development are among his research interests.
Email: d200180179@student.ums.ac.id

Appendix I

S. No.	Abbreviation	Description
1	AFM	Atomic Force Microscopy
2	AM	Additively Manufactured
3	AMMCs	Al Metal Matrix Composites
4	Al	Aluminum
5	ASTM	American Standard Testing and Material
6	C	Coconut Charcoal
7	CMC	Ceramic Matrix Composites
8	Cu	Copper
9	EDS	Energy Dispersive X-ray Spectroscopy
10	EDX	Energy Dispersive X-Ray
11	EELS	Electron Energy Loss Spectroscopy
12	Fe	Iron
13	Mg	Magnesium
14	MMC	Metal Matrix Composites
15	PM	Powder Metallurgy
16	PMC	Polymer Matrix Composites
17	SEM	Scanning Electron Microscopy
18	SEM-EDX	Scanning Electron Microscope-Energy Dispersive X-Ray Spectroscopy
19	Si	Silicon